Available online at www.sciencedirect.com

ScienceDirect

Green Energy & Environment 1 (2016) 84–90

www.keaipublishing.com/gee

Research paper

Cosensitization process effect of D-A-π-A featured dyes on photovoltaic performances

Bo Liu [a,b], Qipeng Chai [a], Weiwei Zhang [a], Wenjun Wu [a], He Tian [a], Wei-Hong Zhu [a,*]

[a] *Shanghai Key Laboratory of Functional Materials Chemistry, Key Laboratory for Advanced Materials and Institute of Fine Chemicals, Collaborative Innovation Center for Coal Based Energy (i-CCE), School of Chemistry and Molecular Engineering, East China University of Science and Technology, Shanghai 200237, China*

[b] *College of Chemistry and Material Science, Hebei Normal University, No. 20, East Road of Nan Er Huan, Shijiazhuang 050023, China*

Received 2 January 2016; accepted 3 February 2016
Available online 6 April 2016

Abstract

Cosensitization based on two or multiple dyes as "dye cocktails" can hit the target on compensating and broadening light-harvesting region. Two indoline D-A-π-A motif sensitizers (**WS-2** and **WS-39**) that possess similar light response area but distinctly reversed feature in photovoltaic performance are selected as the specific cosensitization couple. That is, **WS-2** shows quite high photocurrent but low photovoltage, and **WS-39** gives relatively low photocurrent but quite high photovoltage. Due to the obvious "barrel effect", both dyes show medium PCE around 8.50%. In contrast with the previous cosensitization strategy mostly focused on the compensation of light response region, herein we perform different cosensitization sequence, for taking insight into the balance of photocurrent and photovoltage, and achieving the synergistic improvement in power conversion efficiency (PCE). Electronic impedance spectra (EIS) indicate that exploiting dye **WS-39** with high V_{OC} value as the primary sensitizer can repress the charge recombination more effectively, resulting in superior V_{OC} rather than using dye **WS-2** with high J_{SC} as the primary sensitizer. As a consequence, a high PCE value of 9.48% is obtained with the delicate cosensitization using **WS-39** as primary dye and **WS-2** as accessory dye, which is higher than the corresponding devices sensitized by each individual dye (around 8.48–8.67%). It provides an effective optimizing strategy of cosensitization how to combine the individual dye advantages for developing highly efficient solar cells.

Keywords: Indoline dye; Cosensitization; Adsorption sequence; Charge recombination; Photovoltaic performances

1. Introduction

Dye sensitized solar cells (DSSCs) have attracted widespread attentions as an alternative solar-to-electricity conversion due to their relatively high efficiency and low cost [1–8]. The high requirement for the practical application of DSSCs is always focused on the improvement in power conversion efficiency (PCE) and long-term stability [9–16]. Recently, significant progress has been made on the basis of D-A-π-A motif organic photosensitizers and over 10% PCE has been realized, including porphyrin dyes and pure organic dyes [17–27]. However, even such highly efficient photosensitizers, there is still absorbance valley in visible region. To capture all visible solar light, considerable efforts have been focused on molecular engineering of sensitizers, but few panchromatic sensitizers are obtained with satisfied photovoltaic performance [28–33]. Considering the tediously synthetic work, the specific cosensitization of two or more kinds of dyes as "cocktails" with complementary in absorption spectra becomes a preferably convenient and promising

* Corresponding author.
E-mail address: whzhu@ecust.edu.cn (W.H. Zhu).

http://dx.doi.org/10.1016/j.gee.2016.04.003

method to pursue full or broad solar light harvesting DSSC device [34–38].

Due to the strong absorption band around 450 and 650 nm but extremely weak absorption in region of 350–410 nm and 500–600 nm, porphyrin dyes have been selected as the most promising candidate for cosensitization, which possess complementary light absorption ranges with pure organic dyes [39–44]. By now, the most successful cosensitization was performed between porphyrin dye **YD2-*o*-C8** and pure organic dye **Y123**, along with record power conversion efficiency (PCE) of 11.9% in 2011 [39]. However, even as efficient as **YD2-*o*-C8**, there is still an obvious valley in its IPCE action spectrum from 500 to 650 nm due to the low harvesting efficiency (LHE). Thus, the triphenylamine dye **Y123** was utilized as the cosensitizer to overcome the poor light utilization in this region. Through cosensitization, the PCE was further enhanced to 12.3% [39]. Many other porphyrin dyes were also tried to cosensitize with small molecular organic dyes and obtained high PCE values of over 10%, such as **XW4** and **C1** (10.45%) [34], **XW4** and **XS3** (10.75%) [43], and **LD-31** and **AN4** (10.3%) [44]. Except for porphyrin derivatives, cosensitization between pure organic dyes, especially for indoline dyes, has also been explored and obtained promising PCE improvements [35–38]. It is indicative that the cosensitization strategy is a very effective way to obtain highly efficient DSSCs with lower cost when compared with the synthesis of panchromatic sensitizers. However, all above cosensitization couples were always selected on basis of the complement of absorption spectrum.

Previously, we developed two indoline dyes based on D-A-π-A feature for DSSCs, coded as **WS-2** [45] and **WS-39** [46] (Fig. 1), showing quite different photovoltaic performance. Under the same condition using in this work, with benzothiadiazole as the auxiliary acceptor, **WS-2** showed quite high short-circuit current (J_{SC}) of 18.89 mA cm^{-2} but low open-circuit voltage (V_{OC}) of 636 mV. In contrast, with benzotriazole as the auxiliary acceptor, **WS-39** gave relatively low J_{SC} of 16.75 mA cm^{-2} but quite high V_{OC} of 758 mV. Due to the obvious "barrel effect", the PCE values of both organic sensitizers were only around 8.50%. Accordingly, in this work, to fill up the respective "short board" of two dyes, cosensitization was considered with these two dyes. In contrast with the previous cosensitization strategy mostly focused on the compensation of light response region, we performed different stepwise cosensitization process, and utilized the high J_{SC} **WS-2** and high V_{OC} **WS-39** as the cosensitized couple from viewpoint of combining their respective advantages, especially for exploring the synergistic enhancement for J_{SC} and V_{OC}. As demonstrated, in the cosenstization couple, the V_{OC} values were effectively affected by the adsorption sequence. Further electronic impedance spectra (EIS) reveals that exploiting dye **WS-39** with long alkyl group and high V_{OC} value as the primary sensitizer can repress the charge recombination of the cosensitized cell device more effectively, which provides an optimization strategy for further cosensitized DSSCs.

2. Experimental

2.1. Fabrication of photovoltaic devices

The photoanode was preliminarily prepared by screen printing method with commercial colloidal paste (Dyesol 18NR-T) layer (12 μm) and scattering layer (4 μm), respectively. Followed by a calcination of 500 °C under an air flow for 30 min, the nanoparticles could generate a tight connectivity and a network channel, facilitating electron transport and collection. After a treatment of 0.04 M $TiCl_4$ and a further calcination, the films were cooled down and immersed into single component dye bath or cocktail solutions for stepwise adsorption or mixed solution adsorption, respectively. Subsequently, the counter electrode was obtained by spin coating technique with 0.02 M H_2PtCl_6 in isopropanol solution and sintered under 400 °C for 15 min. Eventually, the two electrodes were sealed with thermoplastic Surlyn, and an electrolyte solution was introduced via one predrilled hole in the counter electrode to finish the sandwiching type-solar cells. The used liquid electrolyte is Z960, with a composition of 0.3 M I_2, 0.1 M GuSCN, 0.5 TBP, 0.05 M LiI and 1.0 M DMImI in actonitrile/valeronitrile (v:v = 85:15) solutions. The active area for working electrodes used in this work was 0.12 cm^2 controlled by a mask with certain area.

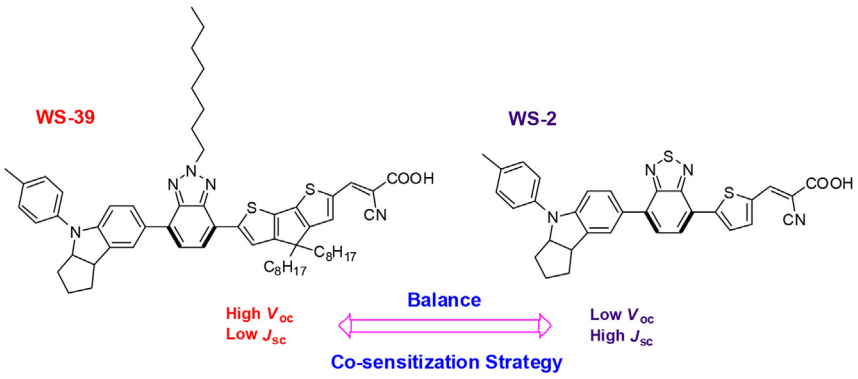

Fig. 1. Photovoltaic optimization with cosensitization strategy based on D-A-π-A featured sensitizers **WS-2** and **WS-39**.

2.2. Characterization

The UV–vis spectra in solutions and on film states were characterized by Cary 100 spectrophotometer. The photocurrent-voltage (I–V) curves were measured under standard AM1.5G simulated solar light by illuminating the device through the FTO substrate from the photoanode side. The incident photon-to-charge carrier efficiencies (IPCEs) were obtained on a Newport-74125 system (Newport instruments). Electronic impedance spectra (EIS) measurements were performed with an impedance analyzer (Solartron Analytical, 1255B) using DSSC devices under 20 °C in the dark. The applied frequency range is 10^{-1}–10^{5} Hz, and the bias potential varied in the range of 0.55–0.75 or 0.45–0.65 V, respectively, with about 25 or 50 mV progressive increase, and the EIS spectra was characterized with Z-View software.

3. Results and discussion

3.1. Coadsorption effect on light-harvesting

Given that the cosensitization was performed in nanoporous state, we initially compared the TiO_2 film properties of two indoline dyes based on D-A-π-A feature, coded as **WS-2** and **WS-39** (Fig. 1). Considering the adsorption performance of dye **WS-2** and **WS-39** on TiO_2 film, the anti-aggregation property of **WS-39** have been previously well documented upon coadsorption with different concentration of CDCA, which can be ascribed to the grafted long alkyl chain [46–48]. In regard with previous cosensitization, we shed light on the adsorption sequence especially for exploring the synergistic enhancement for J_{SC} and V_{OC}. Dye **WS-39** was firstly selected as a primary dye sensitizer, and kept the adsorption process lasted for 12 h, thus resulting in an intense response signal observed around 500 nm (Fig. 2a). Subsequently, the 3-μm TiO_2 films were thoroughly cleaned and dipped into the bath of accessory dye **WS-2** for another 1 or 2 h, respectively. As expected, the absorption valley around 400 nm could be filled and the response signal at longer wavelength could be effectively extended with dipping time from 1 to 2 h (Fig. 2a). However, the ICT peak intensity at around 490 nm was also decreased to considerable extent, implying that there existed the adsorption replacement between two sensitizers, especially for 2 h-dipping. The change tendency on 10 μm-TiO_2 thicker films (Fig. 2b) was similar to that on thinner films, except for the enhanced absorption intensity and extended absorption region owing to more dye uptake on thicker films. In contrast, using **WS-2** as primary dye sensitizer and **WS-39** as accessory dye, the response curves for reversed sequence adsorption on 3 or 10 μm-TiO_2 films were also checked (Fig. 2c and d). After 12 h adsorption of primary dye **WS-2**, two distinct transition bands were observed. Subsequent incorporation of accessory dye **WS-39** leaded to a slight hypochromic shift along with an enhanced ICT signal at around 500 nm, which could be ascribed to the narrower spectra and higher molar extinction coefficient of **WS-39**. To be noticed, both two coadsorption sequences exhibit the similar light-harvesting characteristic through compensating absorption of each dye. Moreover, both **WS-2** and **WS-39** can display excellent stability in DSSCs due to incorporation of auxiliary acceptor, effectively separating the charge distribution in the whole molecule [17,18]. Thus, the stability of the DSSCs will not be obviously influenced by different sequence of cosensitization.

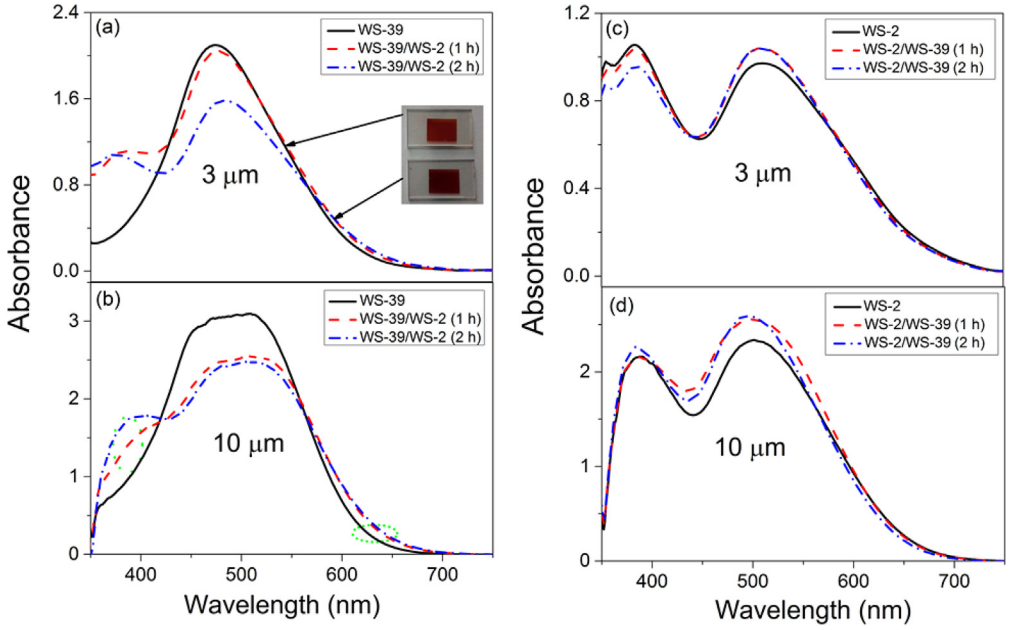

Fig. 2. Absorption spectra of different adsorption sequences: using **WS-39** as primary dye sensitizer and **WS-2** as accessory dye, first sensitized with **WS-39**, and then cosensitized with **WS-2** for 1 or 2 h on 3 μm (a) and 10 μm (b) TiO_2 electrodes; using **WS-2** as primary dye sensitizer and **WS-39** as accessory dye, first sensitized with **WS-2**, and then cosensitized with **WS-39** for 1 or 2 h on 3 μm (c) and 10 μm (d) TiO_2 electrodes.

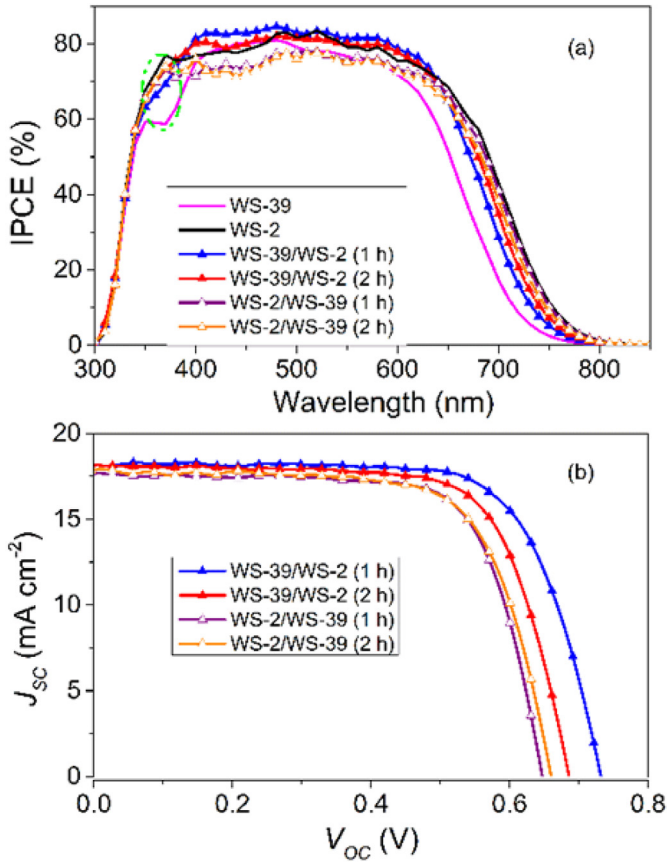

Fig. 3. IPCE action spectra (a) and characteristic I–V curves (b) under various stepwise adsorption conditions.

3.2. Coadsorption sequence effect on photovoltaics

As shown in Fig. 3a, the single **WS-39**-sensitized DSSCs exhibited efficient IPCE values in broad region of 390–610 nm (over 70%), but leaving a response valley around 360 nm, as well as showing inferior response capability toward longer wavelength. This leaves much room for cosensitization strategy. Upon coadsorption with **WS-2** as accessory dye for 1 h, abbreviated as **WS-39/WS-2** (1 h), not only the IPCE value at 370 nm was effectively improved from 58% to 70% due to the stronger absorbance of **WS-2** in this area, but all values in whole IPCE spectrum were also improved. Interestingly, although the absorbance in region of 420–560 nm was declined along with the cosensitization of **WS-2**, the light harvesting capability of cosensitized TiO_2 electrode was still strong enough to capture all the light. It is indicative that the cosensitization using **WS-39** as primary dye and **WS-2** as accessory dye can distinctly improve the light conversion capability, which is consistent with the short-circuit photocurrent (J_{SC}) values of two individual dye. As a result, after 1 h cosensitization with **WS-2**, the J_{SC} value was distinctly increased from 16.75 mA cm^{-2} to a high value of 18.25 mA cm^{-2} (Table 1, **WS-39/WS-2** (1 h)). However, the J_{SC} value was not always increased along with the cosensitization of **WS-2**.

Table 1
Photovoltaic parameters of individual dye-sensitized and cosensitized devices with reversed adsorption sequence.

Devices	J_{SC} (mA cm^{-2})	V_{OC} (mV)	*FF*	PCE
WS-39	16.75	758	0.683	8.67
WS-39/WS-2 (1 h)	18.25	731	0.710	9.48
WS-39/WS-2 (2 h)	18.18	686	0.709	8.84
WS-39/WS-2 (4 h)	17.59	669	0.701	8.26
WS-39/WS-2 (8 h)	15.72	667	0.700	7.34
WS-2	18.89	636	0.706	8.48
WS-2/WS-39 (1 h)	17.69	647	0.721	8.25
WS-2/WS-39 (2 h)	17.76	660	0.703	8.23
WS-2/WS-39 (4 h)	18.02	666	0.697	8.36
WS-2/WS-39 (8 h)	16.93	674	0.702	8.01

While the cosensitization was lasted for one more hour in **WS-39/WS-2** (2 h), the $IPCE_{370\ nm}$ was further increased to around 73%, which was quite similar with the value of DSSC device sensitized by single **WS-2** (76%). Meanwhile, along with the increase of the IPCE values, the onset wavelength of the IPCE action spectra were also red-shifted by around 20 and 26 nm while the cosensitization of **WS-2** was lasted for 1 and 2 h, respectively. To be noticed, although the $IPCE_{370\ nm}$ and the action area could be further improved by extending the cosensitization term, the IPCE values in the range of 400–640 nm in **WS-39/WS-2** (2 h) were slightly decreased compared to those of device in **WS-39/WS-2** (1 h), which was consistent with the change tendency of absorption spectra (Fig. 2b), thus resulting in a slightly decrease of J_{SC} from 18.25 to 18.18 mA cm^{-2}. By the same token, when the dipping time was continually extended to 4 and 8 h, J_{SC} values were further decreased to 17.59 and 15.72 mA cm^{-2}, respectively. Compared with the small J_{SC} difference (ΔJ_{SC}, −0.07 mA cm^{-2}) between **WS-39/WS-2** (2 h) and **WS-39/WS-2** (1 h), the ΔJ_{SC} between **WS-39/WS-2** (4 h) and **WS-39/WS-2** (2 h) and ΔJ_{SC} between **WS-39/WS-2** (8 h) and **WS-39/WS-2** (4 h) were determined to be −0.59 and −1.87 mA cm^{-2}, respectively. That means although the cosensitization of **WS-2** with high J_{SC} could effectively improve the J_{SC} performance from 16.75 to 18.25 mA cm^{-2}, this improvement would vanish gradually along with the extension of the cosensitization, indicating the importance in the process optimization.

In contrast, when the coadsorption sequence of two dyes was reversed (using **WS-2** as primary dye and **WS-39** as accessory dye), the changing trend in J_{SC} was also studied. After a normal 12 h adsorption of **WS-2**, an extremely high J_{SC} of 18.89 mA cm^{-2} was observed. With the cosensitization of **WS-39** for 1 h, abbreviated as **WS-2/WS-39** (1 h), the J_{SC} value was slightly decreased to 17.69 mA cm^{-2} due to the adsorption replacement of **WS-2** (Fig. 3a). While the cosensitization was prolonged to 2 and 4 h, the J_{SC} values were determined to be 17.76 and 18.02 mA cm^{-2} (Table 1), respectively. As a result, the J_{SC} in **WS-39/WS-2** series still remained slightly superior with respect to **WS-2/WS-39** devices.

Except for the J_{SC}, the V_{OC} was also critically dependent upon the cosensitization process of two dyes. While the

cosensitization time of **WS-2** increased from 0 to 8 h (Table 1), the corresponding V_{OC} values of **WS-39/WS-2** series (**WS-39** as primary dye) were first slightly decreased from 758 (0 h) to 731 mV (1 h) and then sharply decreased to 686 (2 h), 669 (4 h), and 667 mV (8 h), respectively, because the **WS-39** with high V_{OC} was replaced by **WS-2**. In case of **WS-2/WS-39** series (**WS-2** as primary dye), the V_{OC} values showed gradual enhancement with the extended cosensitization time of **WS-39**, from 636 (0 h) to 647 (1 h), 660 (2 h), 666 (4 h), and 674 mV (8 h), respectively. Actually, when carefully comparing the photovoltaic parameters of two kinds of devices, although **WS-2/WS-39** series devices showed similar J_{SC} values as **WS-39/WS-2** series devices (around 18.00 mA cm^{-2}), the V_{OC} values were relatively lower, leading to a poor PCE of 8.36% with a J_{SC} of 18.02 mA cm^{-2}, a V_{OC} of 666 mV, and a fill factor (FF) of 0.697, which was even lower than those of individual dye. That means the V_{OC} value was seriously affected by the cosensitization sequence of the dyes. As known, with use of fixed redox species, the V_{OC} is only determined by the Fermi level (E_{Fn}) of TiO_2, which is affected by the conduction band of TiO_2 (E_{CB}) and the charge recombination rate. Thus, to fully understand the change on V_{OC}, the electronic impedance spectra (EIS) results of both kinds of devices were investigated in detail.

3.3. EIS investigation

Five devices fabricated with **WS-39/WS-2** cosensitized TiO_2 electrode were evaluated firstly. The fitted capacitive (C_μ) response [47–49] of five devices was shown in Fig. 4a.

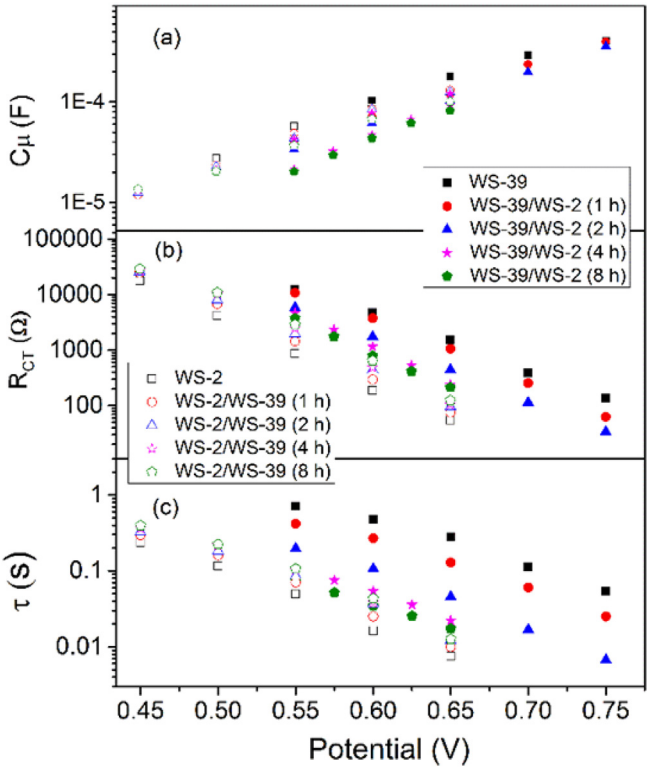

Fig. 4. Plot curves under a series potential bias of DSSCs based on reference dye **WS-39**, **WS-2**, and cosensitization of **WS-39** and **WS-2**: cell capacitance (C_μ, a), recombination resistance (R_{CT}, b), and calculated electron lifetime (τ, c).

The logarithm of C_μ was increased linearly with the given bias potential, and all five curves exhibited the same slope. At fixed potential, device sensitized by **WS-39** presented the highest C_μ value among five devices. Notably, along with the cosensitization of **WS-2**, the C_μ values showed an obvious decay, especially for those of **WS-39/WS-2** (4 h) and **WS-39/WS-2** (8 h). That suggested that when the dipping time was extended, the E_{CB} values would be gradually downshifted, which would decrease the V_{OC} value. Moreover, the recombination resistance (R_{CT}) values were further measured (Fig. 4b). At fixed potential, R_{CT} values of five devices lay in the same order as C_μ values. That is, both C_μ and R_{CT} values of five devices were decreased along with the cosensitization of **WS-2**, being in good agreement with their V_{OC} values (Table 1). Moreover, as shown in Fig. 4c, at fixed potential, taking 0.60 V for example, the electron lifetime (τ) values of five devices were calculated to be 0.48, 0.27, 0.11, 0.05, and 0.03 s, respectively. Obviously, the replacement of **WS-39** by the coadsorbent **WS-2** would gradually accelerate the charge recombination process, thus resulting in the decrease of V_{OC} from 758 to 667 mV.

In case of **WS-2/WS-39** cosensitized DSSC devices, just reverse variation trend was found in EIS measurements. Five devices showed similar capacitive response under the given bias potential, suggesting that the E_{CB} would not be obviously affected while using **WS-39** as the cosensitizer [50,51]. Furthermore, in contrast with **WS-39/WS-2** series devices, at a fixed potential, R_{CT} values of five devices slightly increase as extending the cosensitization time of **WS-39**. However, even the best R_{CT} value of **WS-2/WS-39** series devices was still lower than the poorest result of **WS-39/WS-2** series devices (Fig. 4b). Therefore, the calculated τ values of **WS-2/WS-39** devices were generally shorter than those of **WS-39/WS-2** devices. That means although the charge recombination could be repressed with the cosensitization of **WS-39** to some extent, the overall charge recombination rate was still much faster with respect to **WS-39/WS-2** devices. As a result, the V_{OC} performance of **WS-2/WS-39** devices varied only around 660 mV. Obviously, by using **WS-39**, containing the long alkyl group in π-bridge linker as the primary sensitizer, the charge recombination could be repressed effectively, and the cosensitized devices could succeed superior V_{OC} performance from **WS-39**. As an overall result of J_{SC} and V_{OC}, the DSSC device first sensitized by **WS-39** for 12 h and then cosensitized by **WS-2** for 1 h presented the best power conversion efficiency (PCE) of 9.48% with a J_{SC} of 18.25 mA cm^{-2}, a V_{OC} of 731 mV, and a fill factor (FF) of 0.710, which was obviously higher than that of the individual devices sensitized by either **WS-39** (8.67%) or **WS-2** (8.48%) under the same conditions.

4. Conclusions

Two indoline D-A-π-A sensitizers, possessing distinctly reversed feature in photovoltaic performance, were selected and applied as the cosensitization couple. Through the systematic investigation of cosensitization sequence, two kinds of cosensitized DSSCs with similar light response area but quite

different photovoltaic performance were observed, especially on V_{OC}. EIS measurements indicated that when the dye with long alkyl group and high V_{OC} value (**WS-39**) was used as the primary sensitizer, the charge recombination could be repressed more effectively, and the obviously superior V_{OC} performance could be obtained rather than using the dye with high J_{SC} value (**WS-2**) as the primary sensitizer. As a result, a high PCE value of 9.48% was obtained by **WS-39/WS-2** cosensitized DSSC device, which was higher than that of devices sensitized by each individual dye (around 8.50%). Our work well demonstrates the effective strategy of cosensitization to combine the advantages in photovoltaic parameter of individual dye. More importantly, the optimization effect of cosensitization process on photovoltaic performances affords significant value for future development of highly efficient cosensitization DSSCs.

Conflict of interest

The authors declare no conflict of interest.

Acknowledgments

This work was supported by NSFC for Creative Research Groups (21421004) and Distinguished Young Scholars (21325625), NSFC/China, Oriental Scholarship, Fundamental Research Funds for the Central Universities (WJ1416005 and WJ1315025), Scientific Committee of Shanghai (14ZR1409700 and 15XD1501400), Programme of Introducing Talents of Discipline to Universities (B16017), Science Foundation for the Excellent Youth Scholars of Hebei Education Department (Y2012017), and Science Foundation for Oversea Scholars of Hebei (C201400324).

References

[1] B. O'Regan, M. Grätzel, Nature 353 (1991) 737–740.
[2] A. Hagfeldt, G. Boschloo, L. Sun, L. Kloo, H. Pettersson, Chem. Rev. 110 (2010) 6595–6663.
[3] P. Ganesan, A. Yella, T.W. Holcombe, P. Gao, R. Rajalingam, S.A. Al-Muhtaseb, M. Grätzel, M.K. Nazeeruddin, ACS Sustain. Chem. Eng. 3 (2015) 2389–2396.
[4] Y.K. Eom, I.T. Choi, S.H. Kang, J. Lee, J. Kim, M.J. Ju, H.K. Kim, Adv. Energy Mater. 5 (2015) 1500300.
[5] C. Chou, F. Hu, H. Yeh, H. Wu, Y. Chi, J.N. Clifford, E. Palomares, S. Liu, P. Chou, G. Lee, Angew. Chem. Int. Ed. 53 (2014) 178–183.
[6] B. Xu, E. Sheibani, P. Liu, J. Zhang, H. Tian, N. Vlachopoulos, G. Boschloo, L. Kloo, A. Hagfeldt, L. Sun, Adv. Mater. 26 (2014) 6629–6634.
[7] T. Higashino, Y. Fujimori, K. Sugiura, Y. Tsuji, S. Ito, H. Imahori, Angew. Chem. Int. Ed. 127 (2015) 9180–9184.
[8] X. Lu, T. Lan, Z. Qin, Z. Wang, G. Zhou, ACS Appl. Mater. Interfaces 6 (2014) 19308–19317.
[9] L. Cabau, C. Vijay Kumar, A. Moncho, J.N. Clifford, N. Lopez, E. Palomares, Energy Environ. Sci. 8 (2015) 1368–1375.
[10] K. Kakiage, Y. Aoyama, T. Yano, K. Oya, J. Fujisawa, M. Hanaya, Chem. Commun. 51 (2015) 15894–15897.
[11] Q. Tao, Y. Xia, X. Xu, S. Hedström, O. Bäcke, D.I. James, P. Persson, E. Olsson, O. Inganäs, L. Hou, W. Zhu, E. Wang, Macromolecules 48 (2015) 1009–1016.
[12] W. Tan, R. Wang, M. Li, G. Liu, P. Chen, X. Li, S. Lu, H.L. Zhu, Q. Peng, X. Zhu, W. Chen, W.C.H. Choy, F. Li, J. Peng, Y. Cao, Adv. Funct. Mater 24 (2014) 6540–6547.
[13] S. Kelkar, K. Pandey, S. Agarkar, N. Saikhedkar, M. Tathavadekar, I. Agrawal, R.V.N. Gundloori, S. Ogale, ACS Sustain. Chem. Eng. 2 (2014) 2707–2714.
[14] K. Lim, C. Kim, J. Song, T. Yu, W. Lim, K. Song, P. Wang, N. Zu, J. Ko, J. Phys. Chem. C 115 (2011) 22640–22646.
[15] L. Yang, Z. Zheng, Y. Li, W. Wu, H. Tian, Z. Wang, Chem. Commun. 51 (2015) 4842–4845.
[16] X. Kang, J. Zhang, D. O'Neil, A.J. Rojas, W. Chen, P. Szymanski, S.R. Marder, M.A. El-Sayed, Chem. Mater. 26 (2014) 4486–4493.
[17] Y.Z. Wu, W.H. Zhu, S.M. Zakeeruddin, M. Grätzel, ACS Appl. Mater. Interfaces 7 (2015) 9307–9318.
[18] Y.Z. Wu, W.H. Zhu, Chem. Soc. Rev. 42 (2013) 2039–2058.
[19] A. Yella, C.-L. Mai, S.M. Zakeeruddin, S.-N. Chang, C.-H. Hsieh, C.-Y. Yeh, M. Grätzel, Angew. Chem. Int. Ed. 53 (2014) 2973–2977.
[20] Q.P. Chai, W.Q. Li, J.C. Liu, Z.Y. Geng, H. Tian, W.H. Zhu, Sci. Rep. 5 (2015) 11330.
[21] R. Grisorio, L. De Marco, C. Baldisserri, F. Martina, M. Serantoni, G. Gigli, G.P. Suranna, ACS Sustain. Chem. Eng. 3 (2015) 770–777.
[22] S. Chaurasia, J.S. Ni, W.I. Hung, J.T. Lin, ACS Appl. Mater. Interfaces 7 (2015) 22046–22057.
[23] P.P. Dai, L. Yang, M. Liang, H.H. Dong, P. Wang, C.Y. Zhang, Z. Sun, S. Xue, ACS Appl. Mater. Interfaces 7 (2015) 22436–22447.
[24] X.G. Li, Z.W. Zheng, W. Jiang, W.J. Wu, Z.H. Wang, H. Tian, Chem. Commun. 51 (2015) 3590–3592.
[25] J. Shi, Z.F. Chai, R.L. Tang, J.L. Hua, Q.Q. Li, Z. Li, Sci. China Chem. 58 (2015) 1144–1151.
[26] Y. Jiang, C. Cabanetos, M. Allain, P. Liu, J. Roncail, J. Mater. Chem. C 3 (2015) 5145–5151.
[27] Z.Y. Yao, M. Zhang, R.Z. Li, L. Yang, Y.N. Qiao, P. Wang, Angew. Chem. Int. Ed. 54 (2015) 5994–5998.
[28] M.K. Nazeeruddin, P. Péchy, T. Renouard, S.M. Zakeeruddin, R. Humphry-Baker, P. Comte, P. Liska, L. Cevey, E. Costa, V. Shklover, L. Spiccia, G.B. Deacon, C.A. Bignozzi, M. Grätzel, J. Am. Chem. Soc. 123 (2001) 1613–1624.
[29] C.J. Qin, A. Mirloup, N. Leclerc, A. Islam, A. El-Shafei, L.Y. Han, R. Ziessel, Adv. Energy Mater. 4 (2014) 1400085.
[30] S.W. Wang, C.C. Chou, F.C. Hu, K.L. Wu, Y. Chi, J.N. Clifford, E. Palomares, S.H. Liu, P.T. Chou, T.C. Wei, T.Y. Hsiao, J. Mater. Chem. A 2 (2014) 17618–17627.
[31] Y. Hua, J. He, C.S. Zhang, C.J. Qin, L.Y. Han, J.Z. Zhao, T. Chen, W.Y. Wong, W.K. Wong, X.J. Zhu, J. Mater. Chem. A 3 (2015) 3103–3112.
[32] T. Swetha, S. Niveditha, K. Bhanuprakash, S.P. Singh, Electrochim. Acta 153 (2015) 343–351.
[33] J.J. Li, X.C. Yang, M. Cheng, M. Wang, L.C. Sun, Dyes Pigment. 116 (2015) 58–64.
[34] Y.Q. Wang, B. Chen, W.J. Wu, X. Li, W.H. Zhu, H. Tian, Y.S. Xie, Angew. Chem. Int. Ed. 53 (2014) 10779–10783.
[35] K. Pei, Y.Z. Wu, H. Li, Z.Y. Geng, H. Tian, W.H. Zhu, ACS Appl. Mater. Interfaces 7 (2015) 5296–5304.
[36] M. Rudolph, T. Yoshida, H. Miura, D. Schlettwein, J. Phys. Chem. C 119 (2015) 1298–1311.
[37] K. Kakiage, Y. Aoyama, T. Yano, K. Oya, T. Kyomen, M. Hanaya, Chem. Commun. 51 (2015) 6315–6317.
[38] G. Li, M. Liang, H. Wang, Z. Sun, L.N. Wang, Z.H. Wang, S. Xue, Chem. Mater. 25 (2013) 1713–1722.
[39] A. Yella, H.-W. Lee, H.N. Tsao, C. Yi, A.K. Chandiran, Md. K. Nazeeruddin, E.W.-G. Diau, C.-Y. Yeh, S.M. Zakeeruddin, M. Grätzel, Science 334 (2011) 629–634.
[40] Y.C. Chang, C.L. Wang, T.Y. Pan, S.H. Hong, C.M. Lan, H.H. Kuo, C.F. Lo, H.Y. Hsu, C.Y. Lin, E.W.G. Diau, Chem. Commun. 47 (2011) 8910–8912.
[41] S.K. Das, B. Song, A. Mahler, V.N. Nesterov, A.K. Wilson, O. Ito, F. D'Souza, J. Phys. Chem. C 118 (2014) 3994–4006.

[42] S. Mathew, A. Yella, P. Gao, R. Humphry-Baker, B.F.E. Curchod, N. Ashari-Astani, I. Tavernelli, U. Rothlisberger, Md. K. Nazeeruddin, M. Grätzel, Nat. Chem. 6 (2014) 242−247.
[43] X. Sun, Y.Q. Wang, X. Li, H. Ågren, W.H. Zhu, H. Tian, Y.S. Xie, Chem. Commun. 50 (2014) 15609−15612.
[44] C.L. Wang, J.Y. Hu, C.H. Wu, H.H. Kuo, Y.C. Chang, Z.J. Lan, H.P. Wu, E.W.G. Diau, C.Y. Lin, Energy Environ. Sci. 7 (2014) 1392−1396.
[45] W.H. Zhu, Y.Z. Wu, S.T. Wang, W.Q. Li, X. Li, J. Chen, Z.S. Wang, H. Tian, Adv. Funct. Mater. 21 (2011) 756−763.
[46] Q.P. Chai, W.Q. Li, Y.Z. Wu, K. Pei, J.C. Liu, Z.Y. Geng, H. Tian, W.H. Zhu, ACS Appl. Mater. Interfaces 6 (2014) 14621−14630.
[47] Y.S. Xie, Y.Y. Tang, W.J. Wu, Y.Q. Wang, J.C. Liu, X. Li, H. Tian, W.H. Zhu, J. Am. Chem. Soc. 137 (2015) 14055−14058.
[48] W.Q. Li, Y.Z. Wu, Q. Zhang, H. Tian, W.H. Zhu, ACS Appl. Mater. Interfaces 4 (2012) 1822−1830.
[49] N. Koide, A. Islam, Y. Chiba, L. Han, J. Photochem. Photobiol. A 182 (2006) 296−305.
[50] J. van de Lagemaat, N.G. Park, A.J. Frank, J. Phys. Chem. B 104 (2000) 2044−2052.
[51] S.H. Fan, X.F. Lu, H. Sun, G. Zhou, Y.J. Chang, Z.S. Wang, Phys. Chem. Chem. Phys. 18 (2016) 932−938.